We are IntechOpen, the world's leading publisher of Open Access books Built by scientists, for scientists

4,800
Open access books available

122,000
International authors and editors

135M
Downloads

Our authors are among the

154
Countries delivered to

TOP 1%
most cited scientists

12.2%
Contributors from top 500 universities

CLARIVATE ANALYTICS BOOK CITATION INDEX INDEXED

WEB OF SCIENCE™

Selection of our books indexed in the Book Citation Index in Web of Science™ Core Collection (BKCI)

Interested in publishing with us?
Contact book.department@intechopen.com

Numbers displayed above are based on latest data collected.
For more information visit www.intechopen.com

1

Anisotropy in Woven Fabric Stress and Elongation at Break

Radko Kovar
Technical University of Liberec
Czech Republic

1. Introduction

Anisotropy is a characteristic of most fabrics, especially woven; the impact of the direction of loading on tensile properties can be enormous and is frequently examined, for example in (Dai & Zhang, 2003; Hu, 2004; Kilby, 1963; Kovar & Dolatabadi, 2009; Kovar, 2003; Lo & Hu, 2002; Pan & Yoon, 1996; Postle et al., 1988 etc.). Anisotropy of properties comes out of anisotropy of the structure, based on longitudinal fibers. For woven fabric there are two principal directions – warp and weft (fill), in which yarns and majority of fibres are oriented. Load in principal directions results in minimum breaking elongation and maximum initial modulus. For arbitrary load direction the values of tensile properties change and fabric deformation becomes more complex, often incorporating fabric shear and bend deformation.

Although weave anisotropy is well known, tensile properties are usually theoretically and experimentally investigated namely for principal directions; the main reason is probably complexity of deformation and stress distribution when the load is put at non-principal direction. In this section we shall try to make a step to describe and perhaps to overcome some of these problems.

In practical use, the fabrics are often imposed load in arbitrary direction, bi-axial load or complex load composed of elongation, bend, shear and lateral compression. To predict tensile properties becomes more and more important with development of technical textiles.

Now only main difficulties, connected with the topic of this section, will be outlined:

a. At diagonal load great lateral contraction occurs. It causes complex distribution of stresses. It results in stress concentration at jaws when experiment in accordance with EN ISO 13934-1 is used.
b. There are yarns cut ends in the sample where tensile stress starts from zero.
c. Shear deformation causes jamming of yarns, what can change yarn properties. Strength of the yarn in the fabric can be higher than the strength of free yarn.

There are not available many publications, based on real fabric structure and solving the problem of woven fabric tensile properties in different directions. The reason is mentioned long range of problems and difficulties. Monographs (Hearle et al., 1969 and Postle et al., 1988) are involved in problems of bias fabric load only marginally. (Hu, 2004) is oriented on influence of direction on properties such as tensile work, tensile extension, tensile linearity etc. and uses another approach. Fabric shear at bias extension is investigated in (Du & Yu, 2008). Model of all stress-strain curve of fabric, imposed bias load, is introduced for example in (King, M. J. et al., 2005) with the respect to boundary conditions (stress concentration at

jaws). In (Peng & Cao, 2004) is area of fabric sample separated into 3 zones with different characteristics of bias deformation. Experimental models of woven fabric deformation in different directions are presented by (Zouari et al., 2008). Often the mechanics of continuum approach, coming out of prediction of Hook's law validity, is used, for example, in (Du & Yu, 2008; Hu, 2004; Peng & Cao, 2004 and Zheng et al., 2008). A new method of anisotropy measuring is proposed by (Zheng, 2008) etc.
This section is oriented first of all on anisotropy of rupture properties of weaves, imposed uniaxial load in different directions. The main goal is to develop algorithm for calculation of plain weave fabric breaking strain and stress under conditions of simulated idealized experiment. There are two ways of ideal uni-axial woven fabric loading (details are in section 2): (a) Keeping stable lateral (i.e. perpendicular to direction of load) dimension, (b) Keeping lateral tension on zero (i.e. allowing free lateral contraction).
In this chapter rupture properties will be analyzed for plane weave structure.

2. Nomenclature

β_0, β – angle of warp yarns orientation to the load direction before and after load [rad].
γ – shear angle [rad].
ε – relative elongation or strain [1].
μ – yarn packing density, a share of volume of fibrous material and volume of yarn [1].
ν – Poisson's ratio [1]
b – width of the fabric sample [m].
c – yarn crimp [1]
d – diameter of yarn [m].
F – force [N].
h_0, h – length of the fabric, taken for calculation, before and after fabric elongation [m].
l_0, l – length of the yarn in a crimp wave [m].
L_0, L – projection of the length of the yarn in fabric plane before and after load [m].
s_0, s – component of yarn length L into direction perpendicular to load [m].
p – spacing of yarns (pitch) [m].
S – fabric sett (yarn density) [m^{-1}].
t – fabric thickness [m^{-1}].
T – yarn linear density [Mtex].
Main subscripts: y – yarn, f – fabric, 1 – warp yarn or direction of warp yarns, 2 – weft yarn or direction of weft yarns, 1,2 – warp or weft yarns, 0 – status before load (relaxed fabric), b – status at break, d – diagonal direction (45 ^{o}), n – not-broken yarn, h – horizontal or weft direction, v – vertical or warp direction.

3. Models of woven fabrics rupture properties

Modelling always means simplification of reality and, in our case, idealizing the form of the load. When we wish to simulate experimental investigation of similar property, we should start with brief description of standard fabric rupture properties measuring with the use of EN ISO 13934-1 (strip test) standard. Fast jaws keep the sample in original width (width before load) what results in tension concentration at these jaws. Break usually occurs near the sample grip sooner then real fabric strength is reached. In Fig. 1 a, b are these critical points of the sample marked by circles.

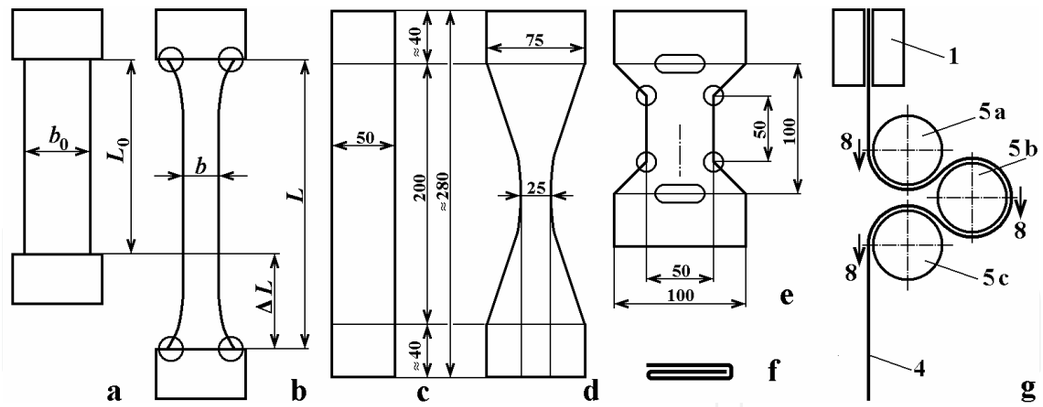

Fig. 1. Tension concentration at jaws and methods of its elimination

There are two main ways how to avoid the problem of tension concentration that occurs when using standard method; sample dimensions are in Fig. 1 c. First is reduction of fabric tension at jaws by narrowing the sample in central part, Fig. 1 d (Zborilova & Kovar, 2004) and 1 e (CSN standard 80 0810). This solution improves the results but some places with tension concentration stay. Till now the best results provides a new method (Kovar & Dolatabadi, 2010), Fig. 1 g; details of the method will be described in section 4.1.

When we wish to model fabric rupture properties and to avoid the problems with uneven tension distribution, we need to analyze a part of the fabric imposed constant load. Virtually there are two idealized situations:

a. To prevent sample from lateral contraction, i.e. to keep the fabric at original width b_0. This can simulate an experiment with infinite fabric width, when the influence of the sample margins becomes negligible. Restriction of lateral contraction must be, in practical experiments, connected with biaxial load, because some complementary load arises in the direction perpendicular to the direction of main load.
b. To allow free lateral contraction of the fabric. This model can simulate an experiment with flexible jaws that change the width simultaneously with fabric lateral contraction, or partly infinite fabric length, where the effect of fast jaws will not change sample relative elongation at break. This model is more complicated owing to fabric jamming and cut ends of yarns under load. Tensile stress in yarn at the cut end is zero and increases gradually due to yarn-to-yarn friction.

Yarn parameters and properties

From parameters and properties of yarn are, for fabric tensile properties investigation, most important: (a) Yarn cross-section as variable parameter. For simplification we can use yarn diameter d. For rough estimation of d can be used well known formula (1), where ρ is density of fibrous material and μ is average yarn packing density, the most problematic parameter. Its average value in free yarn used to be around $\mu_0 \approx 0.5$. This could be used for fabric with low packing density (lose fabric). At tight fabric yarn cross-section becomes flat and packing density increases. Here can be used effective yarn diameter d_{ef}. It is variable parameter, described as distance of yarns neutral axes in cross-over elements. In tight fabric can packing density reach, near warp and weft yarn contact, approximately $\mu_{ef} \approx 0.8$. In fabric near the break, mainly at diagonal load, yarn packing density reaches maximum possible value $\mu_b \approx 0.9$. (b) Yarn stress-strain curve, which can be for some purposes replaced by yarn breaking stress F_{yb} (strength) and strain ε_{yb}. Due to yarn jamming breaking

stress can increase and strain decrease. (c) Unevenness of yarn geometry and other properties. In this section this will be neglected.

$$d = \sqrt{\frac{4T}{\pi \cdot \rho \cdot \mu}}, \quad d_{ef} = \sqrt{\frac{4T}{\pi \cdot \rho \cdot \mu_{ef}}} \tag{1}$$

3.1 Model for infinite sample width

Restriction of lateral contraction makes the models relatively simple. This model and its experimental verification have been described in (Kovar & Gupta 2009). A conception of this theory is the test with infinite sample width that does not allow fabric lateral contraction. Experimental verification was based on keeping the tubular sample in original width by two fast wires (see Fig. 19). The yarns in model fabric are shown in Fig. 2; 1 is upper jaw, 2 bottom jaw before and 3 after elongation or at break.

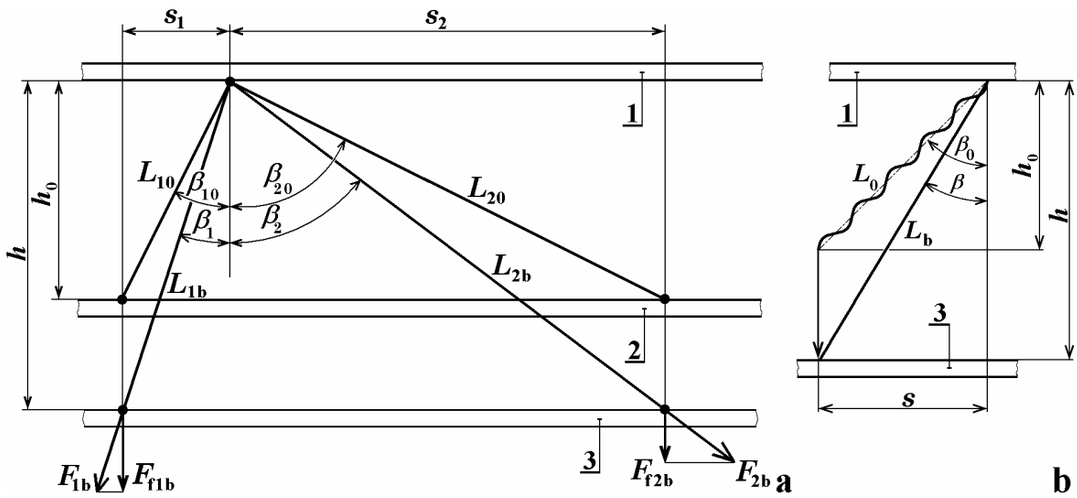

Fig. 2. Warp and weft yarns dimensions before load and at break

Relative fabric elongation, ε_f, and warp and weft yarns elongations, $\varepsilon_{1,2}$, are defined as

$$\varepsilon_f = \frac{h - h_0}{h_0} = \frac{h}{h_0} - 1 \text{ and } \varepsilon_{1,2} = \frac{L_{1,2b} - L_{1,20}}{L_{1,20}} = \frac{L_{1,2b}}{L_{1,20}} - 1 \tag{2}$$

Original lengths of warp L_{10} and weft L_{20} yarns before elongation between the jaws are

$$L_{10} = \frac{h_0}{\cos\beta_{10}} \text{ and } L_{20} = \frac{h_0}{\cos\beta_{20}} = \frac{h_0}{\sin\beta_{10}} \tag{3}$$

where β_0 is the angle between direction of warp or weft yarns and direction of load. After fabric elongation from h_0 on h yarn angles decrease from $\beta_{1,20}$ to $\beta_{1,2}$.

Note: subscripts 1, 2 denotes validity of expression either for warp or for weft yarns, valid are either the first or the second subscripts, so often one expression contains two equations.

The final lengths of yarns segments will be L_{1b} and L_{2b}. As lateral contraction is restricted, horizontal projections of yarn segments will not change and so $s_{1,2} = s_{1,20}$. Fig. 2 b describes two main means of each yarn elongation, i.e. decrimping and yarn axial elongation.

With the exception of one particular load angle β_0 only one system of yarns reaches breaking elongation; in so called square fabric, when all the parameters are for warp and weft directions the same, first break yarns with β_0 < 45 °. For these broken yarns their lengths at fabric break will be $L_{1,2b} = L_{1,20} \cdot (1 + \varepsilon_{1,2b}) \cdot (1 + c_{1,20})$, where $\varepsilon_{1,2b}$ is yarn relative elongation at break and $c_{1,20}$ is crimp of the yarn, see Fig. 6 and Equation (7). As in this case it is s = const. we shall obtain, using Pythagorean Theorem, the length of the fabric at break $h = \sqrt{L_{1,2b}^2 - s_{1,2}^2}$ and fabric breaking elongation ε_{fb} will be

$$\varepsilon_{fb} = \frac{h}{h_0} - 1 = \frac{\sqrt{\left(L_{1,20} \cdot (1 + \varepsilon_{1,2b}) \cdot (1 + c_{1,20})\right)^2 - s_{1,2}^2}}{h_0} - 1 \tag{4}$$

where $s_{1,2} = h_0 \cdot \tan \beta_{1,20}$.

Characteristics of this formula is shown, for one value of warp yarns extensibility ε_{1b} = 0.2 and five values of weft yarns extensibility ε_{2b} = 0.1; 0.15; 0.2; 0.25 and 0.3, in Figure 3. As it was mentioned, with the exception of one critical angle only yarns of one system (warp ore weft) will break. The critical angle can be found as crossing points of the curves for warp and weft yarns.

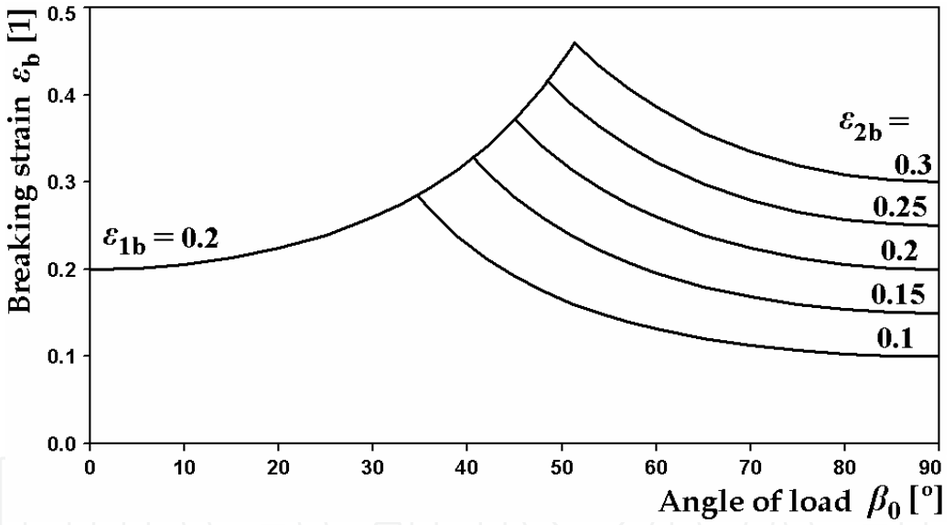

Fig. 3. Influence of angle load on breaking elongation for different yarn

Breaking stress, i.e. force necessary for damage of 1 m width of the fabric, can be calculated as the sum of the stresses from all yarns in 1 m of fabric width. Number of yarns in fabric width unit is $n = n_1 + n_2 = S_1 \cdot \cos \beta_{10} + S_2 \cdot \cos \beta_{20}$, where $S_{1,2}$ are fabric setts. The component of yarns axial stresses to the direction of external load from one broken yarn is $F_{f1,2b} = F_{1,2b} \cdot \cos \beta_{1,2}$ (see Fig. 2), $F_{1,2b}$ is strength of one yarn (axial force at break). The force from one non-broken yarn $F_{1,2n}$ depends on this yarn elongation at fabric break $\varepsilon_{1.2n}$ and on yarn stress-strain curve. For simplification we shall assume linear yarn deformation and so $F_{1,2n} = F_{1,2b} \cdot \frac{\varepsilon_{1,2n}}{\varepsilon_{1,2b}}$. The final result, the force necessary for breakage of 1 m fabric width is

$$F_{fb} = F_{f1,2b} + F_{f2,1n} = F_{1,2b} \cdot \cos\beta_{1,2} \cdot S_{1,2} \cdot \cos\beta_{1,20} + F_{2,1b} \cdot \cos\beta_{2,1} \cdot S_{2,1} \cdot \cos\beta_{2,10} \cdot \frac{\varepsilon_{2,1n}}{\varepsilon_{2,1b}} \quad (5)$$

where $F_{f1,2b}$ is the force in 1 m fabric width from all broken yarns, $F_{f2,1n}$ is the same from non-broken yarns. If change of angle of yarn incline during the elongation is neglected, i.e. if $\beta_{1,2} = \beta_{1,20}$, equation (5) would be simplified as

$$F_{fb} = F_{1,2b} \cdot \cos^2\beta_{1,20} \cdot S_{1,2} + F_{2,1b} \cdot \cos^2\beta_{2,10} \cdot S_{2,1} \cdot \frac{\varepsilon_{2,1n}}{\varepsilon_{2,1b}} \quad (6)$$

Examples of results of calculation are shown in the following charts. In Fig. 4 is set warp and weft yarns extensibility at break, that includes de-crimping and yarns breaking elongation, on $\varepsilon_{1b} = \varepsilon_{2b} = 0.2$, warp yarn strength $F_{1b} = 8$ and weft yarn strengths are variable. Warp and weft yarns set is $S_1 = S_2 = 1000$ m^{-1}. Similarly in Fig. 5 is shown influence of yarn extensibility on fabric breaking stress for $\varepsilon_{1b} = 0.2$, variable ε_{2b}, $F_{1b} = 8$ N and $F_{1b} = 6$ N. In Figs. 4 and 5 thick lines represent calculation according to equation (5) and thin lines follows equation (6).

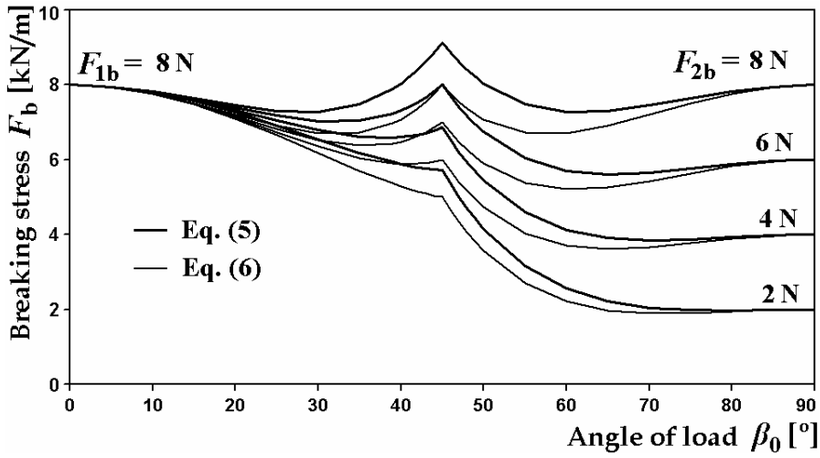

Fig. 4. Influence of angle β_0 on breaking stress for $F_{1b} = 8$ N, different F_{2b}, $\varepsilon_{1b} = \varepsilon_{2b} = 0.2$

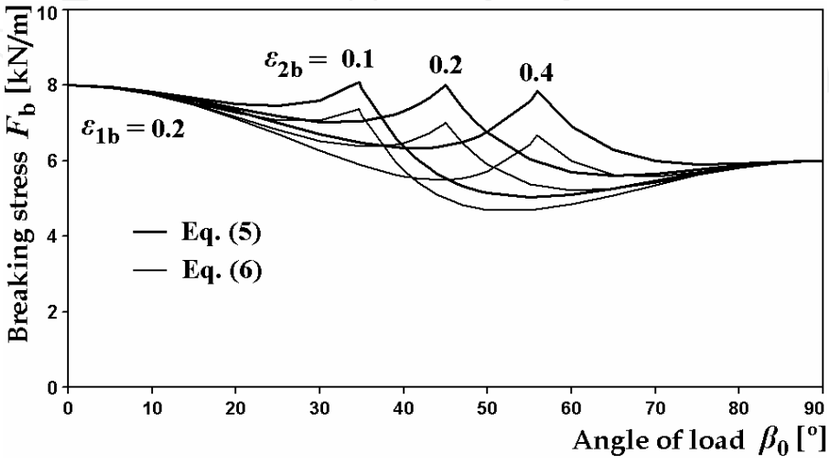

Fig. 5. Influence of angle β_0 on breaking stress for $\varepsilon_{1b} = 0.2$, different ε_{2b}, $F_{1b} = 8$ and $F_{2b} = 6$ N

Figures 3, 4 and 5 show significant peeks at critical angle where lines for warp yarns and weft yarns meet; this is not recognized in experimental results. This disagreement is caused by simplified model approach that assumes ideally even yarn properties. In real fabric, variability in yarn breaking strain and in other parameters causes, near mentioned critical point, break of some warp and some weft yarns together.

3.2 Model for infinite sample length

Models of ideally uni-axial woven fabric load in variable directions are rather complicated, first of all from the next reasons: (a) Substantial change in yarns incline (angle β) toward load direction during fabric elongation results in combination of tensile and shear deformation. The change of angle β allows itself certain fabric elongation and so its diagonal extensibility and lateral contraction is greater. (b) Reduction of yarns crimp in bias directions is limited, whereas at load in principal directions crimp of the yarns, imposed load, could be practically zero. (c) Change in fabric properties caused by jamming of yarns at diagonal load is great. The jamming could improve utilization of fibers strength and so the strength of the yarn could become better than that at load in principal directions. (d) There are cut ends of the yarns, bearing fabric load, what changes the results when the fabric width is limited. In the next steps will be modeled relaxed fabric, fabric at load in principal and in different directions.

3.2.1 Relaxed fabric

Investigation of fabric tensile properties starts at definition of relaxed state. It is described in (Lomov et all, 2007) etc. Simple model of plain weave balanced fabric in shown in Figure 6. Wavelength λ_1 of warp is defined by weft pitch p_2 and vice versa. Fabric thickness is t; average p value corresponds with reciprocal value of fabric sett S of the opposite yarn system and so $\lambda_{1,20} = 2p_{2,10} = \frac{2}{S_{2,10}}$. Main parameters of crimp wave are: wavelength λ, wave amplitude a and length of the yarn axis l. Wave amplitudes a are dependent on yarn diameters and in non-square fabric (i.e. $S_1 \neq S_2$, $d_{10} \neq d_{20}$, $l_{10} \neq l_{20}$ etc.) as well on fabrics setts, yarns diameters, imposed load (contemporary or in fabric history) and so on.

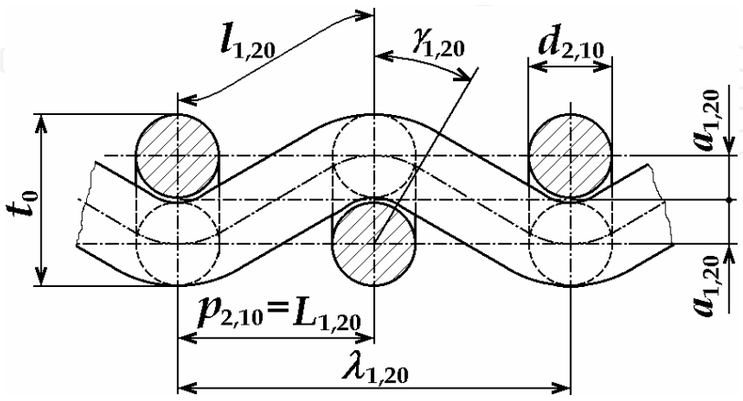

Fig. 6. Definition of yarn crimp in a woven fabric.

Crimp of the yarns in woven fabric as numeric parameter c is defined by equation (7); wavelength of warp λ_1 corresponds with pitch of weft p_2 and vice versa.

$$c_{1,20} = \frac{l_{1,20}}{p_{2,10}} - 1 \quad \text{or} \quad l_{1,20} = \left(c_{1,20} + 1\right) \cdot p_{2,10} \tag{7}$$

Lengths of the yarn in a crimp wave l will be counted with the help of equation (8). This formula approximates crimp c of loose fabrics (low packing density) using sinusoid crimp wave model and of tight fabrics (high packing density) using Pierce's model.

$$c_{1,20} = 2.52 \cdot \left(\frac{a_{1,20}}{p_{2,10}}\right)^2 \quad \text{or} \quad c_{1,2} = 2.52 \cdot \left(\frac{a_{1,2}}{p_{2,1}}\right)^2 \tag{8}$$

Relative crimp wave amplitude a/p can reach maximum value of 0.57735 at so called fabric limit packing density (maximal available fabric sett) for square fabric construction. In Figure 7 is curve, following equation 8, compared with calculation of crimp using sinusoid and Peirce crimp wave models (Kovar & Dolatabadi 2008).

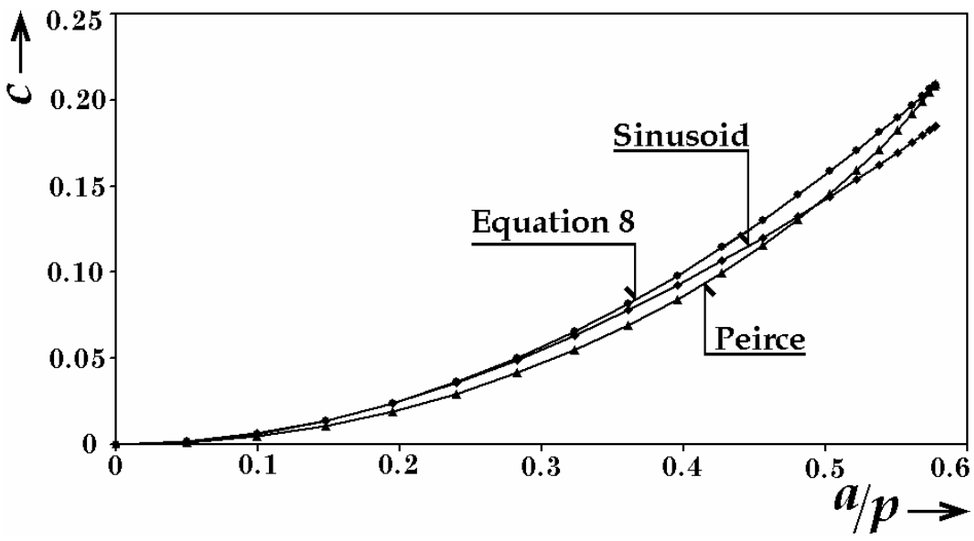

Fig. 7. Dependance of crimp c on relative crimp amplitude a/p.

Using equations 7 and 8 one get for length of the yarn in a crimp wave l:

$$l_{1,20} = \left(2.52 \cdot \left(\frac{a_{1,20}}{p_{2,10}}\right)^2 + 1\right) \cdot p_{2,10} = 2.52 \cdot a_{1,20}^2 + p_{2,10}^2 \quad \text{or} \quad l_{1,2} = 2.52 \cdot a_{1,2}^2 + p_{2,1}^2 \tag{9}$$

Note: equations 7, 8 and 9 are valid both for fabric status before (with subscript 0) and after load. Parameters p_0 are known (reciprocal values of setts S) and height of the crimp wave can be, for square fabric, estimated as $a_{10} = a_{20} = 0.5\ d$.

3.2.2 Load in principal directions

These directions are analyzed in different publications (Hearle et al., 1969; Hu, 2004; Pan, 1996 etc.) sufficiently and so this paragraph will describe only few important parameters.

a. **Fabric breaking force** $F_{f1,2}$ (subscripts 1, 2 specify warp or weft direction of imposed load). For its calculation simple equation (10) can be used (Kovar, 2003), in which $F_{1,2b}$

are breaking forces of one warp or weft yarn and $C_{1,2u}$ are coefficients of utilization of these forces at fabric break. We shall assume, that in principal directions it will be $C_{1,2u} \approx 1$, as there are two opposite tendencies; yarn and fabric unevenness results in decreasing of $C_{1,2u}$ and fabric jamming can, on the contrary, this parameter increase.

$$F_{f1,2} = S_{1,2} \cdot F_{1,2b} \cdot C_{1,2u} \tag{10}$$

b. **Fabric breaking strain**, $\varepsilon_{f1,2}$. There are two main resources of fabric elongation (Kovar & Gupta, 2009): yarn straightening (de-crimp) and yarn axial elongation. For principal direction it will be assumed that all yarns at break are straight and so in equation (8) $a_{1,2} = 0$. For yarn axial elongation experimental results of yarn at breaking strain, $\varepsilon_{1,2b}$, can be used.

$$\varepsilon_{f1,2} = \left(1 + \varepsilon_{1,2b}\right) \cdot \left(1 + c_{1,20}\right) - 1 \tag{11}$$

Explanation: equation (11) can be derived from general definition of relative elongation with the use of (7) and Fig. 6:

$$\varepsilon_{f1,2} = \frac{l_{1,2} - p_{2,10}}{p_{2,10}}, \quad \text{in which} \quad l_{1,2} = p_{2,10} \cdot \left(\varepsilon_{1,2b} + 1\right) \cdot \left(c_{1,20} + 1\right),$$

where $l_{1,2}$ are lengths of the yarn in a crimp wave after straightening and elongation.

c. **Fabric width**. Fabric elongation in principal directions is attached with straightening (de-crimping) of the yarns imposed load, whereas opposite yarns crimp amplitude increases and fabric contracts. We shall assume that lateral contraction is similar as elongation in lateral direction. There are two opposite tendencies again: quicker increase of yarn crimp at greater a/p, Fig. 7, and yarn cross-section deformation (flattening). Original width of the sample b_0 will be changed into $b_{b1,2}$:

$$b_{b1,2} = \frac{b_0}{1 + \varepsilon_{fb1,2}} \text{ and } b_0 = b_{b1,2} \cdot \left(1 + \varepsilon_{fb1,2}\right) \tag{12}$$

d. **Lateral contraction**. Fabric Poisson's ratio ν can be counted using

$$\nu_{1,2} = \frac{b_0 - b_{b1,2}}{b_0} = \frac{b_{b1,2} \cdot \left(1 + \varepsilon_{fb1,2}\right) - b_{b1,2}}{b_{b1,2} \cdot \left(1 + \varepsilon_{fb1,2}\right)} = \frac{\varepsilon_{fb1,2}}{1 + \varepsilon_{fb1,2}} \tag{13}$$

3.2.3 Load in diagonal direction (45 º) for structural unit

Load at diagonal directions is connected with shear deformation and lateral contraction (Sun & Pan, 2005 a, b). This analysis helps with recognition of yarns spacing p_d and angle of yarns incline β_d at fabric break, Fig. 8. Elongation of woven fabric in principal directions is restricted by the yarn system that lays in direction of imposed load, whereas load in angle of 45 º with free lateral contraction enables greater breaking strain thanks to shear deformation. For description of fabric geometry at break it is necessary to describe jamming in the fabric; break can't occur sooner than maximum packing density is reached.

There are two opposite trends for originally circular yarn cross-section change: (a) Fabric lateral contraction is connected with increase of compressive tension between neighboring

yarns. This tension causes tendency to increase the fabric thickness. (b) Crimp of the yarns could not be near zero as it was at loading in warp or weft directions, because now both yarn systems are imposed load. Axial stress in all yarns leads to tendency of de-crimping and so to reduction of fabric thickness.

The situation for initial value of warp and weft yarns decline $\beta_{1,20} = \beta_{d0} = 45°$ is shown in Figure 8 (a before, b after uniaxial elongation), where $p_{1,2} = p_d$ describes yarn perpendicular spacing, p_h and p_v are projections of these parameters in horizontal and in vertical direction, respectively.

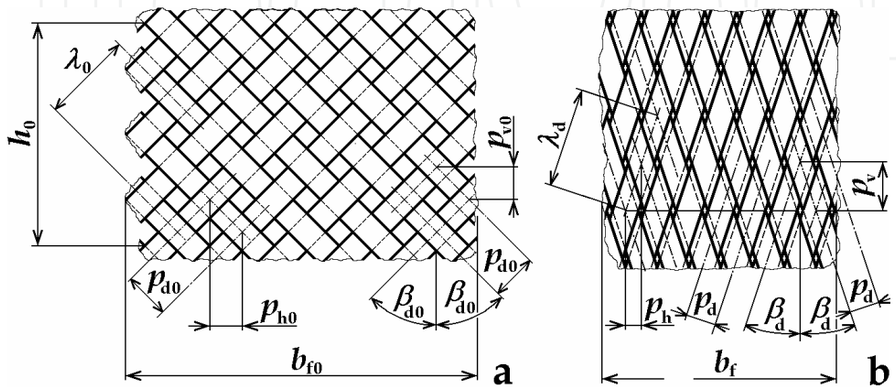

Fig. 8. Diagonal fabric deformation at ideally uniaxial load for $\beta_0 = 45^{o}$ for square fabric.

Spacing of yarns, p_0, is independent parameter corresponding with reciprocal value of fabric sett ($p_0 = 1/S$). During diagonal deformation p decreases and at fabric break it reaches minimum value that restricts fabric lateral contraction and breaking elongation. A hypothesis of even packing density μ distribution in all fabric thickness at break is accepted and so profiles of yarns in crossing points can be as shown in Fig. 9 a for the same material in warp and in weft or in Fig. 8 b for different diameters in warp and weft. Parameter δ, defined as $\delta = \frac{p_d}{t_d}$, can be variable, or another hypothesis of maximum area $p_d \cdot t_d$ can be incorporated and then $\delta = \frac{p_d}{t_d} = 1$ (Figs 9 a and b; Fig. c is for $\delta \neq 1$).

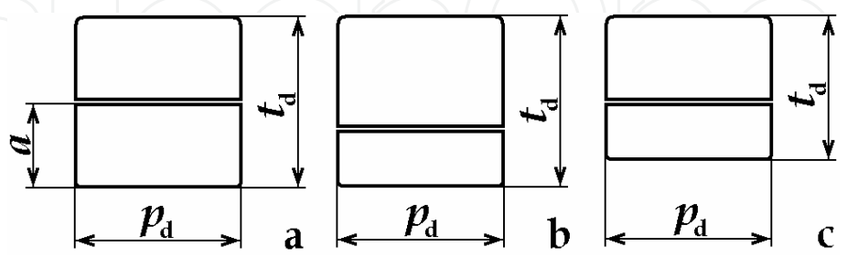

Fig. 9. Model profiles of warp and weft yarns in crossing elements.

If A_0 is original area of warp and weft yarns cross-section at packing density μ_0 ($A_0 = \frac{\pi \cdot \left(d_{10}^2 + d_{20}^2\right)}{4}$, approximately $\mu_0 = 0.5$), final area $A = p_d \cdot t_d$ after yarn compression (at packing density $\mu = 0.8$) will be $A = A_0 \cdot \mu_0/\mu$. Then yarn spacing will be, for $p_d = t_d$:

$$p_d = \frac{A}{p_d} = \frac{A_0 \cdot \frac{\mu_0}{\mu}}{p_d} = \frac{\frac{\pi \cdot \left(d_{10}^2 + d_{20}^2\right)}{4} \cdot \frac{\mu_0}{\mu}}{p_d} \quad \text{and so} \quad p_d = \sqrt{\frac{\pi \cdot \left(d_{10}^2 + d_{20}^2\right)}{4} \cdot \frac{\mu_0}{\mu}} \tag{14}$$

Note: experiments show, that $p_1 = p_2 = p_d$ also for fabric in which $S_1 \neq S_2$. When yarn diameters are different ($d_1 \neq d_2$), then p_1 and p_2, β_1 and β_2 will be different, but these changes will be small.

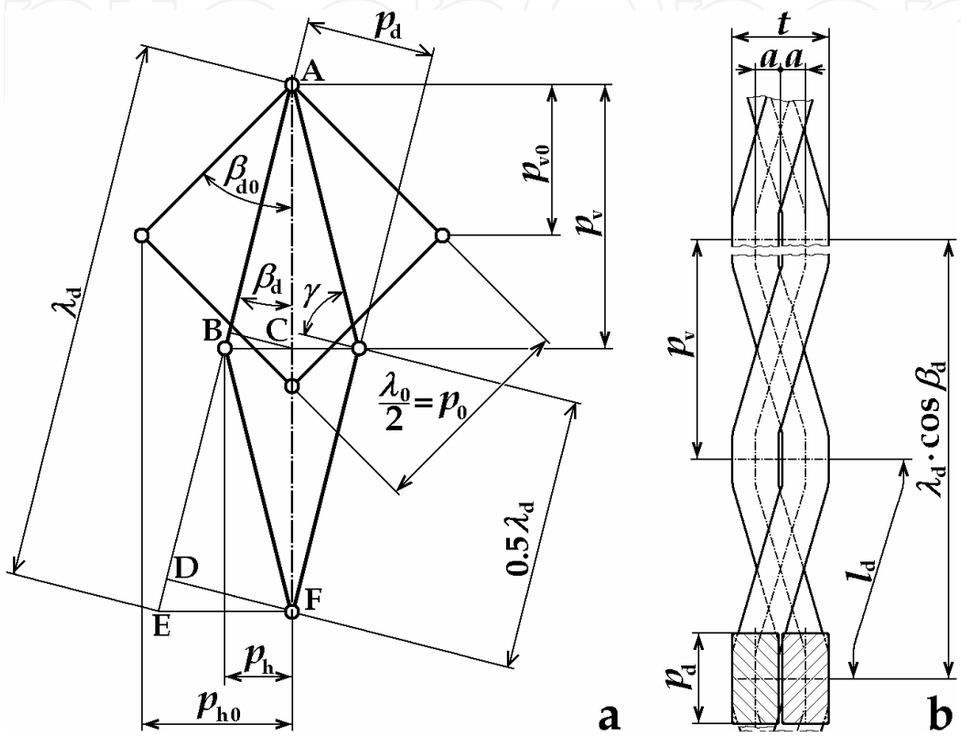

Fig. 10. Geometrical analysis of structural unit deformation at $\beta_0 = 45^\circ$ for square fabric.

Geometrical changes, connected with shear fabric deformation at diagonal load of one fabric structural element (this is a square connecting four adjacent crossing points), are described using Figure 10 a, where β_{d0}, β_d are angles of yarns incline before deformation and at break ($\beta_{d0} = 45^\circ$), γ is shear angle ($\gamma = \frac{\pi}{2} - 2\beta_d$, $\gamma_0 = 0$), p_0, p_d is spacing (pitch) of yarns before and after deformation. Parameter p_0 corresponds with fabric sett and with ½ of wavelength of crimped yarns λ_0 (Figs. 6 and 8). λ_d is wavelength of crimped yarns at break. Elongation of λ_0 is enabled both by yarns straightening and by yarn axial elongation, residual crimp of warp and weft yarns can be counted using parameter $a = 0.5\ t_d = 0.5\ p_d$ (Figures 9, 10 b) or neglected, because for $a/p < 0.1$ is $c < 0.006$, Fig. 7. p_{h0} and p_h are horizontal projections of yarn spacing p_0 and p_d before and after deformation and similarly p_{v0} and p_v are vertical projections of p_0 and p_d before and after deformation; these parameters are necessary for calculation of fabric breaking elongation and of maximum shear angle γ, see as well Fig. 10 b (view in direction perpendicular to the load).

Length of the yarn in a crimp wave, l_d, increases in the course of elongation, but due to jamming not so much as in free yarn. We shall assume that yarn axial elongation at break is reduced on axial elongation at break of fibers ε_{fib} and so it will be, see Fig. 6 and equation (9):

$$l_{1,2\mathrm{d}} = l_{1,20} \cdot \left(1 + \varepsilon_{\mathrm{fib}}\right) = \left(2.52 \cdot a_{1,20}^2 + p_{2,10}^2\right) \cdot \left(1 + \varepsilon_{\mathrm{fib}}\right) \tag{15}$$

Experimentally such yarn breaking elongation can be measured with a very short test length (shorter than is the length of the fibers) to simulate status of fibers and yarn in the fabric.
Getting wavelength of crimped yarn at break, λ_{d}, needs to know crimp wave amplitude a (Figs. 9, 10 b); it is assumed, that $a = \frac{t_{\mathrm{d}}}{4} = \frac{p_{\mathrm{d}}}{4}$. Using crimp definition $c_{1,2} = \frac{l_{1,2}}{p_{2,1}} - 1$ and replacing $p_{2,1}$ for $0.5 \cdot \lambda_{1,2}$ we get $0.5\lambda_{1,2\mathrm{d}} = \frac{l_{1,2\mathrm{d}}}{c_{1,2\mathrm{d}} + 1}$. Parameter $c_{1,2\mathrm{d}}$ can be counted with the help of equation (8): $c_{1,2\mathrm{d}} = 2.52\left(\frac{a}{0.5 \cdot \lambda_{1,2\mathrm{d}}}\right)^2$. After connection and conversion we get quadratic equation $0.5\lambda_{1,2\mathrm{d}}^2 - l_{1,2\mathrm{d}} \cdot 0.5\lambda_{1,2\mathrm{d}} + 2.52 \cdot a^2 = 0$ that leads to the result

$$0.5 \cdot \lambda_{1,2\mathrm{d}} = \frac{l_{1,2\mathrm{d}} + \sqrt{l_{1,2\mathrm{d}}^2 - 4 \cdot 2.52 \cdot a^2}}{2} \tag{16}$$

Using Fig. 10 one can calculate horizontal and vertical projection of the yarn spacing before deformation, p_{h0} and p_{v0}, and after deformation (triangle ABC), p_{h} and p_{v}:

$$p_{\mathrm{h0}} = 0.5 \cdot \lambda_0 \sin\frac{\pi}{4} = 0.5 \cdot p_0 \cdot \sqrt{2} \quad \text{and} \quad p_{\mathrm{h}} = 0.5 \cdot \lambda_{\mathrm{d}} \cdot \sin\beta_{\mathrm{d}} \tag{17}$$

$$p_{\mathrm{v0}} = 0.5 \cdot \lambda_0 \cos\frac{\pi}{4} = 0.5 \cdot p_0 \cdot \sqrt{2} \quad \text{and} \quad p_{\mathrm{v}} = 0.5 \cdot \lambda_{\mathrm{d}} \cdot \cos\beta_{\mathrm{d}} \tag{18}$$

Minimum yarn spacing, p_{d}, has already been known from equation (14). It can help with calculation of p_{v} and p_{h} that give fabric breaking elongation and lateral contraction. From Fig. 10, triangles AEF and DEF, it will be $\sin\beta_{\mathrm{d}} = \frac{2p_{\mathrm{h}}}{\lambda_{\mathrm{d}}}$ and $\sin\beta_{\mathrm{d}} = \frac{p_{\mathrm{d}}}{2p_{\mathrm{h}}}$ and hence $\frac{2p_{\mathrm{h}}}{\lambda_{\mathrm{d}}} = \frac{p_{\mathrm{d}}}{2p_{\mathrm{h}}}$, $p_{\mathrm{h}} = \frac{\sqrt{p_{\mathrm{d}}\lambda_{\mathrm{d}}}}{2}$, what results in angle of yarn incline at break β_{d}:

$$\sin\beta_{\mathrm{d}} = \frac{\sqrt{p_{\mathrm{d}} \cdot \lambda_{\mathrm{d}}}}{\lambda_{\mathrm{d}}} \text{ and } \beta_{\mathrm{d}} = \arcsin\frac{\sqrt{p_{\mathrm{d}} \cdot \lambda_{\mathrm{d}}}}{\lambda_{\mathrm{d}}} \tag{19}$$

Fabric elongation at diagonal break $\varepsilon_{\mathrm{db}}$ is, using eq. (18):

$$\varepsilon_{\mathrm{db}} = \frac{p_{\mathrm{v}} - p_{\mathrm{v0}}}{p_{\mathrm{v0}}} = \frac{\lambda_{\mathrm{d}} \cdot \cos\beta_{\mathrm{d}} - p_0 \cdot \sqrt{2}}{p_0 \cdot \sqrt{2}} \tag{20}$$

Maximum value of shear angle γ_{d} will be $\gamma_{\mathrm{d}} = \frac{\pi}{2} - 2 \cdot \cos\beta_{\mathrm{d}}$

3.2.4 Load in diagonal direction (45 º) for fabric strip

Strip of the tested fabric of original width b_0 at angle of warp and weft yarns decline to vertical load direction $\beta_{10} = \beta_{20} = 45$ º is shown in Figure 11 (a before load, b after load for square fabric, c after load for non-square fabric with $S_1 \neq S_2$ or/and $\varepsilon_{1b} \neq \varepsilon_{2b}$).

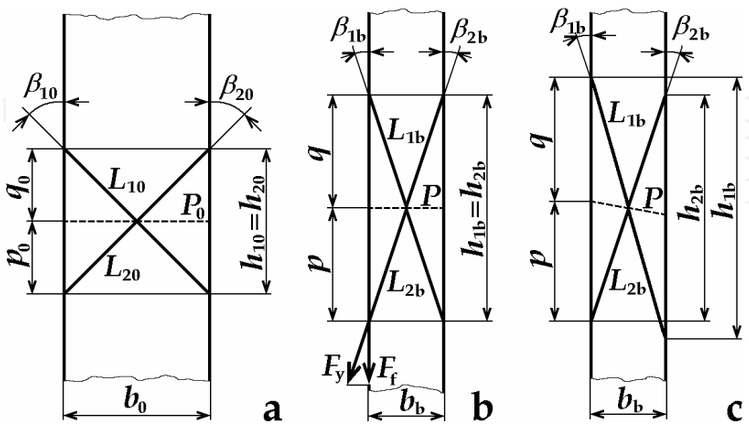

Fig. 11. Geometrical analysis of sample deformation at $\beta_0 = 45$ º.

Lengths of the weft and the warp yarns in fabric plane before elongation, L_{10} and L_{20}, are $L_{1,20} = \dfrac{b_0}{\sin\beta_{1,20}}$, where for $\beta_{10} = \beta_{20} = \beta_0 = 45$ º is $\sin\beta_{1,20} = \dfrac{\sqrt{2}}{2}$. The width of the sample at break, b_b, and fabric lateral contraction, ν, can be counted using equation (17), in which p_h corresponds with b ($\dfrac{p_h}{p_{h0}} = \dfrac{b_b}{b_0}$):

$$b_b = b_0 \cdot \frac{p_h}{p_{h0}} = b_0 \cdot \frac{0.5 \cdot \lambda_d \cdot \sin\beta_d}{p_0 \cdot \sqrt{2}} \text{ and } \nu_b = \frac{b_0 - b_b}{b_0} \tag{21}$$

Note: equation (21) gives, for non-square fabric (Figure 11 c), different results for weft and warp yarns ($b_{1b} \neq b_{2b}$). In this case we shall assume that minimum value of b and maximum value of ν is valid; the reason is that maximum load is only in one yarn system, the opposite systems of yarns with lower or negative load cannot keep fabric strip wider as the yarns are able to bear only negligible compressive load.

Now we shall count fabric breaking elongation, using knowledge of sample width b_b, equation (21), and determination of projections of lengths of the yarns axes l_1 and l_2 into fabric plane L_1 and L_2 (Figs. 6, 11):

$$l_{1,20} = L_{1,20}\left(1 + c_{1,20}\right) \text{ and } l_{1,2b} = l_{1,20}\left(1 + \varepsilon_{fib}\right) = L_{1,20} \cdot \left(1 + c_{1,20}\right) \cdot \left(1 + \varepsilon_{fib}\right) \tag{22}$$

Relation between lengths of yarns axes calculation before load, l_{10} and l_{20}, and at break, l_{1b} and l_{2b}, is described by equation (9). The lengths of yarns axes projection into fabric plane, L_{1db} and L_{2db}, will be from (22)

$$L_{1,2b} = \frac{l_{1,2b}}{1 + c_{1,2b}} = \frac{L_{1,20} \cdot \left(1 + c_{1,20}\right) \cdot \left(1 + \varepsilon_{fib}\right)}{1 + c_{1,2b}} \tag{23}$$

Yarns elongation at break is reduced on the value, corresponding with elongation at break of fibers. Crimp of yarns at break is taken from equation (8), where p is replaced with 0.5 λ:

$$c_{1,2\mathrm{db}} = 2.52 \cdot \left(\frac{a}{0.5 \cdot \lambda_{1,2}} \right)^2 \tag{24}$$

Horizontal projections of lengths $L_{1\mathrm{b}}$ and $L_{2\mathrm{b}}$ are $h_{1,2} = \sqrt{L_{1,2\mathrm{b}}^2 - b_{\mathrm{db}}^2}$.
Finally fabric sample breaking elongation $\varepsilon_{\mathrm{fbd}}$ is (Fig. 11) for $h_{1\mathrm{b}} = h_{2\mathrm{b}} = h_{\mathrm{b}}$ and $h_0 = b_0$:

$$\varepsilon_{\mathrm{fbd}} = \frac{h_{\mathrm{b}} - h_0}{h_0} = \frac{h_{\mathrm{b}} - b_0}{b_0} \tag{25}$$

More complex is breaking elongation calculation for non-square fabric (Fig. 11 c) when $L_1 \neq L_2$. It leads to skewed fabric in which originally horizontal line P_0 will get some another angle to load direction. In this case it could be assumed, that thanks to possibility of reaching new equilibrium, fabric breaking elongation will be average of the values, get from equation (24) for weft and warp yarns; this assumption is in good agreement with experimental results.
Breaking stress of the fabric, F_{fb}, equation (26), can be got by modification of equation (10). The role of both warp and weft yarns strength is for one critical angle $\beta_{0\mathrm{c}}$ identical (for square fabric $\beta_{0\mathrm{c}}$ = 45 °, for other fabrics it is near 45 °). Incline of yarns is as well considered; only component of yarn axial stress F_{y} into direction of fabric load F_{f} supports fabric strength (it is shown in Fig. 11 b). Prediction of coefficients of yarn strength utilization C_{u} is in this case difficult, because due to jamming strength of the yarn can be higher than the strength of free yarn. On the contrary, cut yarn ends causes gradual tensile stress increase from zero at sample edge to maximum value (it will be described later).

$$F_{\mathrm{fb}} = S_1 \cdot F_{1\mathrm{b}} \cdot C_{1\mathrm{u}} \cdot \cos\beta_{1\mathrm{b}} + S_2 \cdot F_{2\mathrm{b}} \cdot C_{2\mathrm{u}} \cdot \cos\beta_{2\mathrm{b}} \tag{26}$$

3.2.5 Load in variable directions – breaking strain

Example for angle of load β_{10} = 30 ° is described in Fig. 12. The lengths of warp and weft yarns projections into fabric plane within the sample width b_0 before elongation, L_{10} and L_{20}, can be counted similarly as in previous paragraph.
For further calculations it is necessary to know sample width b_{b} at break as variable, dependent on angle β_0. We shall assume, in accordance with experimental results, that the change of b is slower near the critical angle $\beta_{0\mathrm{c}}$ ($\beta_{0\mathrm{c}} \approx 45$ °, value of b is here at minimum) and quicker near β_0 = 0 ° and 90 °. This is the reason, why parabolic approximation in equation (27) is used. In this, $b_{1,2\mathrm{b}}$ is sample width at break for angle of load 0 ° or 90 ° and b_{db} is the same for angle of load 45 °.

$$b_{\mathrm{b}}(\beta_0) = (b_{1,2\mathrm{b}} - b_{\mathrm{db}}) \cdot \left(1 - \frac{4}{\pi} \cdot \beta_0 \right)^2 + b_{\mathrm{db}} \tag{27}$$

Sample strain at break is, with the exception of critical angle $\beta_{0\mathrm{c}}$, restricted namely by yarns of one system (warp or weft), usually by that with smaller value of β_0. Elongation at break near $\beta_{0\mathrm{c}}$ is influenced first of all by: (a) Crimp interchange. At mentioned $\beta_{0\mathrm{c}}$ both warp and

weft yarns are crimped and so an important crimp interchange occurs; yarns of one system get straight whereas crimp of the opposite yarns grows. This mechanism enables, in some range of angles β_0, to utilize strength of warp and weft yarns simultaneously. Out of this range, stress in the yarn of the system with greater β_0 becomes negligible or even negative (compression). (b) Effect of yarn jamming, that increases yarn breaking stress, is maximum at β_{0c} and minimum for $\beta_0 = 0^{\circ}$ or 90°.

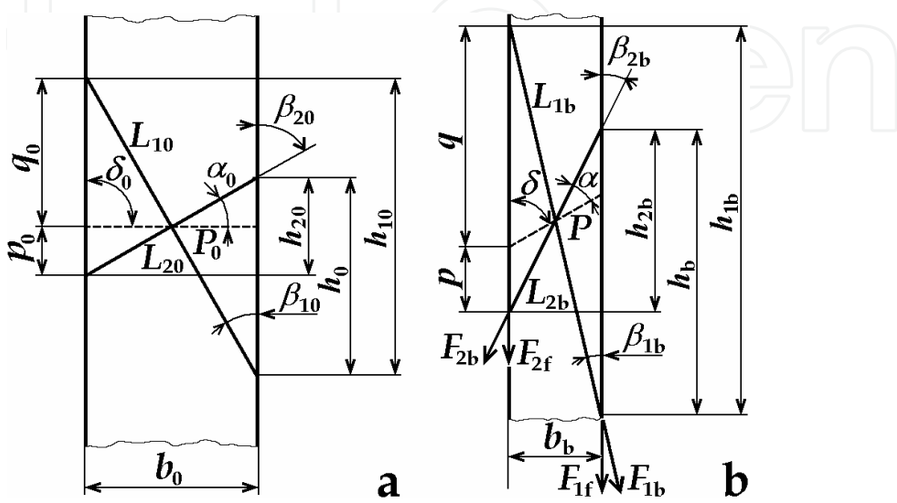

Fig. 12. Deformation of a fabric strip before deformation (a) and at break (b).

One of the results of different stresses in warp and weft yarns is that originally horizontal line P_0 changes after load its direction δ_0 for δ, see Fig. 12 (dash lines) and (Zouari, Amar & Dogui, 2008). Lengths of the yarn axis projections at break, $L_{1,2b}$, corresponding with the lengths $L_{1,20}$ before load, can be counted similarly as in equation (23). Crimps $c_{1,2b}$ are variable near critical angle β_{0c}, near principal directions are crimps of broken yarns neglected. Yarn elongations at break $\varepsilon_{1,2b}$ are as well variable; near angle β_{0c} it is $\varepsilon_{1,2b} = \varepsilon_{fib}$.

$$L_{1,2b} = \frac{L_{1,20} \cdot \left(1 + c_{1,20}\right) \cdot \left(1 + \varepsilon_{1,2b}\right)}{1 + c_{1,2b}} = \frac{b_0 \cdot \left(1 + c_{1,20}\right) \cdot \left(1 + \varepsilon_{1,2b}\right)}{\sin \beta_{1,20} \cdot \left(1 + c_{1,2b}\right)} \tag{28}$$

For fabric breaking strain it is necessary to know vertical projections of $L_{1,2b}$, parameters $h_{1,2b}$ (Fig. 12). Using Pythagorean Theorem and equations (27) and (28) it will be

$$h_{1,2b} = \sqrt{L_{1,2b}^2 - b_b^2} \tag{29}$$

The same parameters before load, $h_{1,20}$, are

$$h_{1,20} = L_{1,20} \cdot \cos \beta_{1,20} \tag{30}$$

Now we can count, separately for warp and weft yarns, fabric breaking elongation, $\varepsilon_{1,2b}$. Smaller of the results will be valid (break yarns of only one system).

$$\varepsilon_{1,2b} = \frac{h_{1,2b} - h_{1,20}}{h_{1,2b}} \tag{31}$$

In Fig. 13 is shown an example of results for calculated and measured breaking elongation. Fabric was plain weave, cotton yarn linear density 35 tex (warp and weft), warp sett 2600 ends/m, weft sett 2500 ends/m, finished fabric. Experiment 1 was carried on in accordance with the standard EN ISO 13934-1, experiment 2 is in accordance with (Kovar & Dolatabadi, 2010).

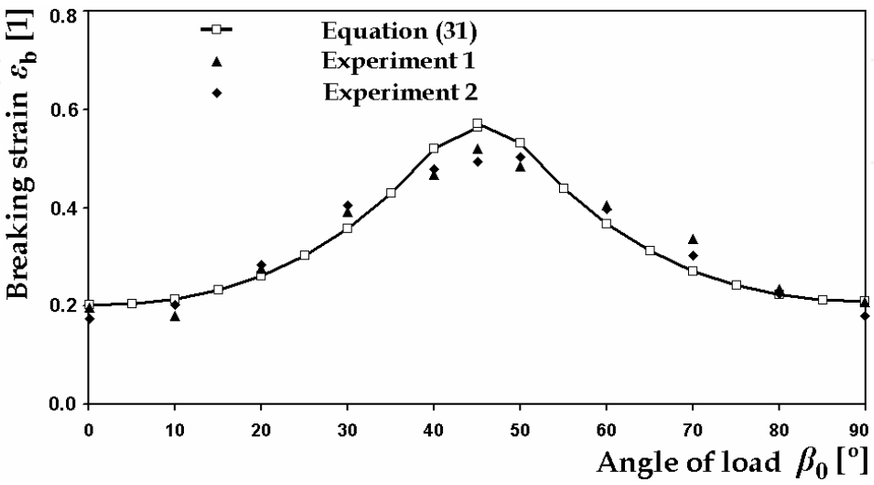

Fig. 13. Example of calculated and measured fabric strain at break.

3.2.6 Load in variable directions – breaking stress

Force from one broken yarn. Basic algorithms for breaking stress calculation were explained sooner, equations (10) and (26). For variable β_0 it is necessary to consider that only component of yarn axial stress F_1 and F_2 aims in direction of load, Fig. 12. Components of axial tensile force of one yarn at fabric break, $F_{1,2b}$, into fabric load direction, $F_{1,2f}$, are $F_{1,2f} = F_{1,2b} \cdot \cos\beta_{1,2b}$, where angles of yarns incline at break $\beta_{1,2b}$ can be counted using (27) and (29):

$$\tan\beta_{1,2b} = \frac{b_b}{h_{1,2b}} \quad \text{and} \quad \beta_{1,2b} = \arctan\frac{b_b}{h_{1,2b}} \tag{32}$$

Force from all broken yarns. Number of broken yarns in fabric width at break corresponds with fabric sett S, width b and angle of load β_0 and so comprehensive force from all warp or weft yarns in fabric strip, $F_{a1,2b}$, is

$$F_{a1,2b} = S_{1,2} \cdot b_0 \cdot \cos\beta_{1,20} \cdot F_{1,2f} = S_{1,2} \cdot b_0 \cdot \cos^2\beta_{1,20} \cdot F_{1,2b} \tag{33}$$

where $n_{1,2} = S_{1,2} \cdot b_0 \cdot \cos\beta_{1,20}$ is number of yarns in sample width.

Correction for fabric jamming

At diagonal load, utilization of fibers strength can be better then at load in principal directions. It will be described by coefficient C_{fu}, equation (10). In this chapter only rough estimation will be presented. Fibers strength utilization, by other words a share of broken fibers to all fibers in yarn cross-section, can be: (a) In free spun yarn around value of C_{fuy} =

0.5; it depends on fibers length (staple), friction coefficients, yarn twist etc. (b) In fabric at break in principal directions, C_{fup} is similar or slightly higher; it depends on fabric packing density and on other parameters. (c) In fabric at break in diagonal directions, C_{fud} is maximal due to jamming. Extremely it can be near to 1. From these reasons, final parameters $C_{fu1,2}$ as a function of β_0, will be predicted as parabolic relation (without derivation):

$$C_{fu1,2}(\alpha_0) = (C_{fud} - C_{fup}) \cdot \left(\frac{\beta_0}{\frac{\pi}{4}} \right)^2 + C_{fup} \tag{34}$$

Fabric strip strength from broken yarns with implementation of jamming, $F_{j1,2b}$, is from (33) and (34):

$$F_{j1,2b} = C_{fu1,2} \cdot F_{a1,2b} = C_{fu1,2} \cdot S_{1,2} \cdot b_0 \cdot \cos^2 \beta_{1,20} \cdot F_{y1,2b} \tag{35}$$

Correction for cut yarn ends

With the exception of $\beta_0 = 0$ and $\beta_0 = 90$ ° there are yarns, bearing fabric load, having one or two free ends (Kovar & Dolatabadi, 2007). Near cut yarn end axial stress is zero and gradually increases (linear increase is assumed) due to friction till it reaches yarn strength in length l, see Fig. 14 a. In this area fabric jamming is not as important as in sample inner parts and shear angle is smaller. This length l is hardly predictable and depends on many parameters (setts, yarn properties including frictional, fabric finishing, shear deformation, angle of load, jamming etc.). It can be evaluated experimentally by testing yarn pullout force from the fabric (Pan & Yoon, 1993) or testing the samples of variable widths. By this effect, some width on each side of fabric $b_{in} = l \cdot \sin \beta_{1,20}$ is inefficient; this is important mainly for broken yarns. This strip b_{in} can bear only about 50 % of full load. It results in reduction of original sample width to effective one $b_{ef} = b_{b0} - l \cdot \sin \beta_{1,20}$.

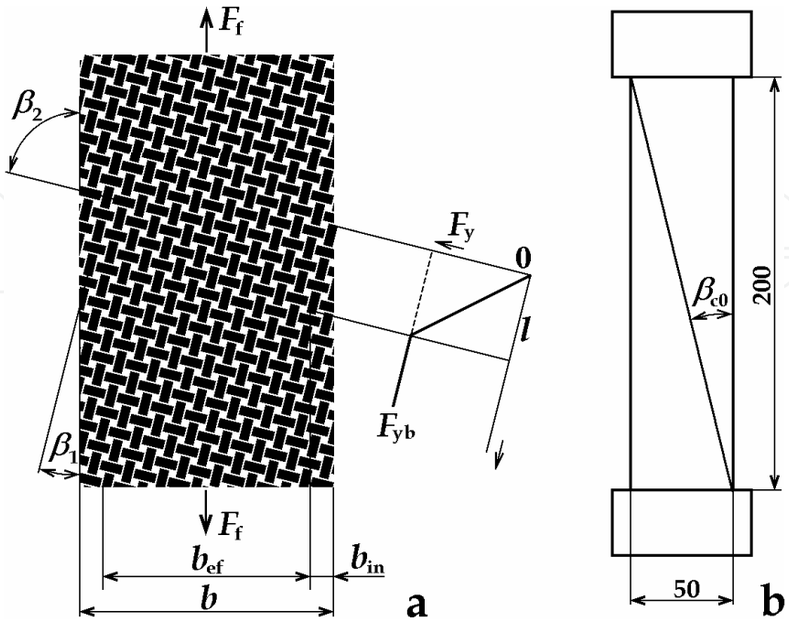

Fig. 14. Free ends of yarns in fabric at bias load.

Total effective force from broken yarns with reduced fabric width, $F_{f1,2b}$, is then from (35)

$$F_{f1,2b} = C_{fu1,2} \cdot S_{1,2} \cdot b_{ef} \cdot \cos^2 \beta_{1,20} \cdot F_{y1,2b} = C_{fu1,2} \cdot S_{1,2} \cdot \left(b_{b0} - l \cdot \sin \beta_{1,20}\right) \cdot \cos^2 \beta_{1,20} \cdot F_{y1,2b} \qquad (36)$$

Correction for critical angles

In our theory, unlimited sample length is assumed and the effect of critical angles is neglected. Nevertheless for comparison with real experiments it should be mentioned; tension concentration at jaws reaches high value for critical angles, at which only 1 yarn is kept simultaneously by both pair of jaws and all others yarns have 1 end free. For critical angle β_{c0} it will be: $\tan \beta_{c0} = 50 : 200$, see Fig. 14 b (sample width is 50 mm, test length 200 mm). Near this angle an important drop in tested fabric strength is observed.

Example of results for plain weave fabric, warp and weft yarns are polypropylene/cotton 35/65 %, linear density T = 29.5 tex, warp sett S_1 = 2360 ends/m, weft sett S_2 = 1920 (lines 1 and 3) and S_2 = 1380 ends/m (lines 2 and 4) is shown in Fig. 15. Lines 3, 4 describes standard experiment (EN ISO 13934-1), lines 1, 2 results of the new method (Kovar & Dolatabadi, 2010) with the same size of samples. Drop in the sample strength near critical angles is evident.

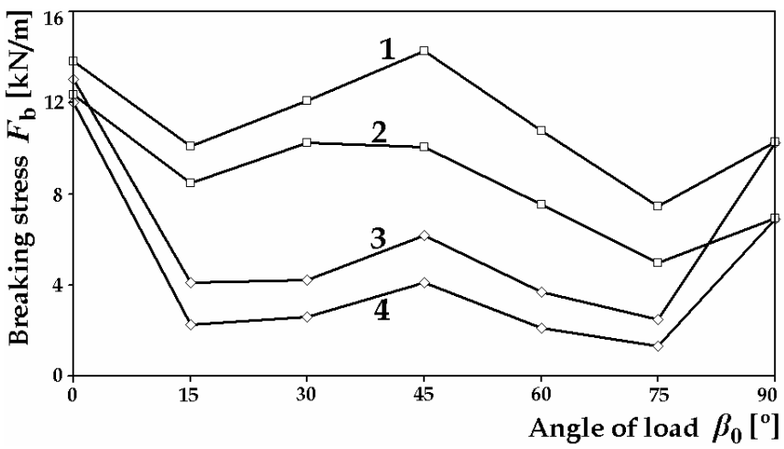

Fig. 15. Influence of critical angles on fabric breaking stress.
Note: linear connection of measured points only assembles these points together; in any case it is does not mean approximation of the results.

Force from unbroken yarns at fabric break

These yarns are, for fabric strength, important only near critical angle β_{0c} (near 45 °). At other load angles, tensile stress in these yarns is low or negative. We shall assume, that maximum force corresponds with maximum length $L_{1,2b}(\beta_0)$, Fig. 12, and that it can be calculated using formula (33) on condition of similar tensile properties of warp and weft yarns.

Vertical projection of unbroken yarn length at fabric break, $h_{u1,2}$, depends on this parameter before load ($h_{1,20}$) and on sample elongation at break (elongation of sample is proportional), identified by broken yarns of the opposite system: $h_{u1,2} = h_{1,20} \cdot \left(1 + \varepsilon_{2,1b}\right)$. Length of unbroken yarns in fabric width before load is $L_{1,20} = \dfrac{b_0}{\sin \beta_{1,20}}$, corresponding length of unbroken yarns at fabric break (Fig. 12), $L_{u1,2}$, is using (29), $L_{u1,2} = \sqrt{b_b^2 + h_{1,2b}^2}$.

Relative elongation of unbroken yarns is then

$$\varepsilon_{u1,2} = \frac{\left(L_{u1,2} - L_{1,20}\right)}{L_{1,20}} \tag{37}$$

and hence force, by which unbroken yarns contribute to sample strength, will be:

$$F_{u1,2b} = F_{a1,2d} \cdot \frac{L_{u1,2}}{L_{u1,20}} \tag{38}$$

where Fa1,2d is breaking load, calculated in accordance with (33) for $\beta 0 = 45$ °.

Final results

Force $F_{12,b}$ is the sum of the forces from broken and unbroken yarns, equations (36) and (38):

$$F_{1,2b} = F_{f1,2b} + F_{u1,2b} \tag{39}$$

In Fig. 16 is an example of results, carried on the same fabric and with the same experimental methods as shown in Fig. 13. Agreement is not excellent; it is caused by simplifications in calculation and as well by imperfection of known experimental methods. Results of patented method (experiment 2, Kovar & Dolatabadi, 2010) shows, with exception of principal directions, higher breaking stress than does standard method (experiment 1, EN ISO 13934-1). Important drop is observed near previously mentioned critical angles β_0 14 and 76 °. Slower decrease of breaking stress near angle β_0 = 45 ° is due to interactions between warp and weft yarns that were not implemented into calculation yet.

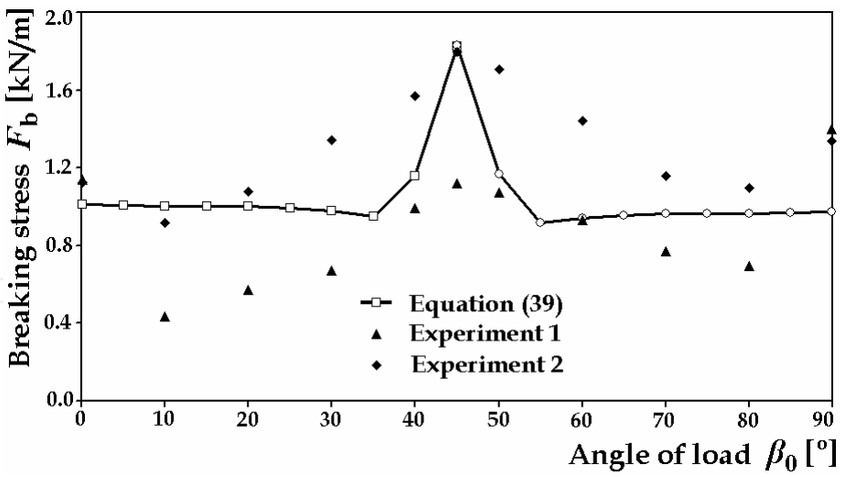

Fig. 16. Example of calculated and measured fabric stress at break.

4. Measuring of rupture properties

Experiments always mean some scale of unification and simplification in comparison with fabric real loading at the use. To simulate real practical situations is not possible – it would result in too many different experimental methods. In general, the load put on textile fabric, can be (a) tensile uniaxial, (b) tensile biaxial or (c) complex as combination of different form

of the load (elongation, bend, shear etc.). Nevertheless uniaxial and biaxial stresses are the most important forms of load for investigation of textile fabrics rupture properties. Other forms of deformation (bending, shear, lateral pressure etc.) seldom result in fabric break.

4.1 Uniaxial stress

The problems, connected with breaking test of woven fabrics due to great lateral contraction that accompanies load in diagonal directions, have already been described in section 2 (Fig. 1). The principle of a new method (Kovar & Dolatabadi, 2010) is sample tension reduction by fabric capstan friction, Fig. 17 (scheme and photographs at three stages of sample elongation). A set of fast cylinders 5, 6 is connected with each pair of dynamometer jaws 1, 2. At sample elongation fabric slips towards central fabric part 4 in directions 8, what results in tension reduction due to capstan friction; however, fabric lateral contraction on cylinders is enabled. Total angle of contact is on each sample side is approximately 8.03 π (460 °) and for friction coefficient f = 0.17 (this is low value of f, valid for fabric to smooth steel surface friction at high load near break of the sample) decrease of sample tension will be $\frac{F_c}{F_j} = e^{\alpha \cdot f} \doteq 3.9$ (390 %). In Fig. 17 right is example of tested sample before elongation (a), at elongation of 40 % (b) and 90 % near the break point (c).

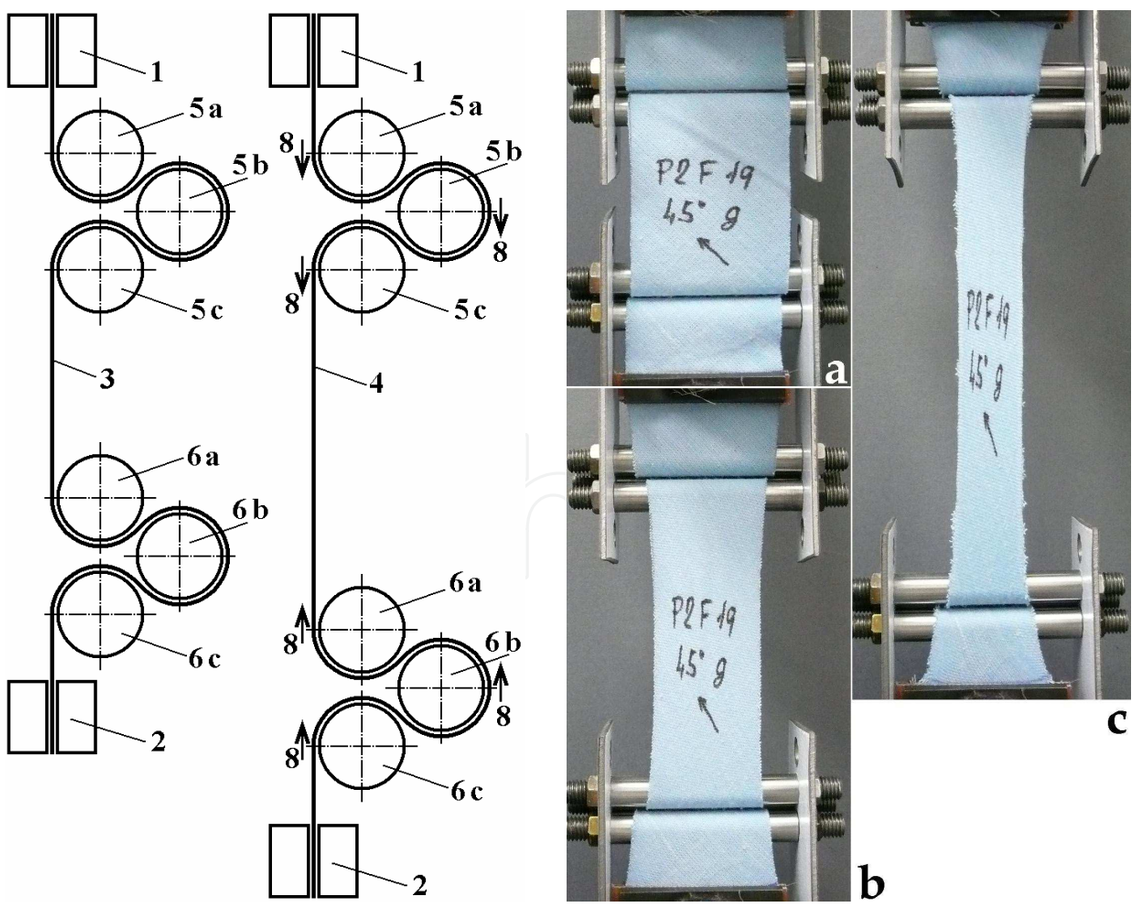

Fig. 17. Patented method for fabric tensile properties measuring

4.2 Biaxial stress

Measuring of fabric tensile properties at biaxial stress is more complicated task, described for example in (Bassett, Postle & Pan, 1999). If fast jaws 1 are used, Fig. 18 a, fabric would soon break at sample corners as relative elongation of L_2 is many times greater than that of sample length and width L_1. MA is measured area of the sample. Two of solutions are shown. In Fig. b are fast jaws replaced with sets of individual narrow free grippers and in Fig. c is measured sample MA connected with four auxiliary fabrics cut into strips that enable 2-D sample elongation, although jaws 1 are fast. Two mentioned methods are suitable for measuring fabric anisotropy, nevertheless they need special equipment and much of labor. It is not easy to investigate rupture properties by these methods. As the load in two directions can be different, it would be useful to reduce number of tested samples by election of only some variants such as: (a) uniaxial load (but different than at standard methods, lateral contraction is now enabled), (b) restriction of lateral contraction similarly with chapter 2.2, (c) the same load (absolutely or recounted per one yarn in the sample width) or tension in two directions, (d) the same elongation in two directions.

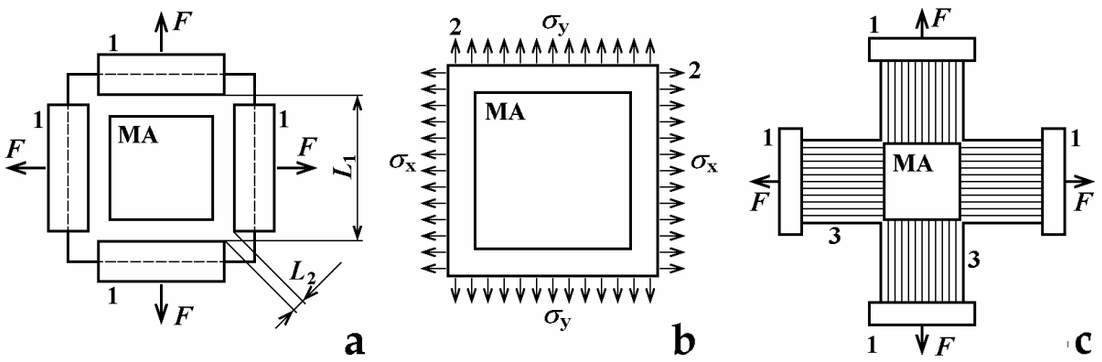

Fig. 18. Principles of tensile properties measuring at biaxial load

The principle of measuring tensile properties when fabric lateral contraction is restricted (simulation of sample infinite width, section 2.1) is shown in Fig. 19. The sample 1 is sewn by several individual stitches into tubular form and by wires 3, placed beside jaws 2, is kept in original width.

5. Discussion, current trends and future challenges in investigated problems

The problems of anisotropy of woven fabric rupture properties are very complex and till now not in the gravity centre of researches. This section could make only a short step in bringing new knowledge on this field. Partly another approach to similar problem solution is used in (Dolatabadi et al., 2009; Dolatabadi & Kovar, 2009). Anisotropy of different fabric properties is often investigated for textile based composites, where rupture properties are very important, for example in (Hofstee & van Keulen, 2000).

There are lots of possibilities how to go on in research on this topic, for example:

a. Investigation of influence of sample width on tensile properties with the goal to specify better impact of cut yarn ends (Fig. 14).
b. Research on biaxial and combined fabric load, the aim could be, for example, better description of fabric behaviour at practical usage.

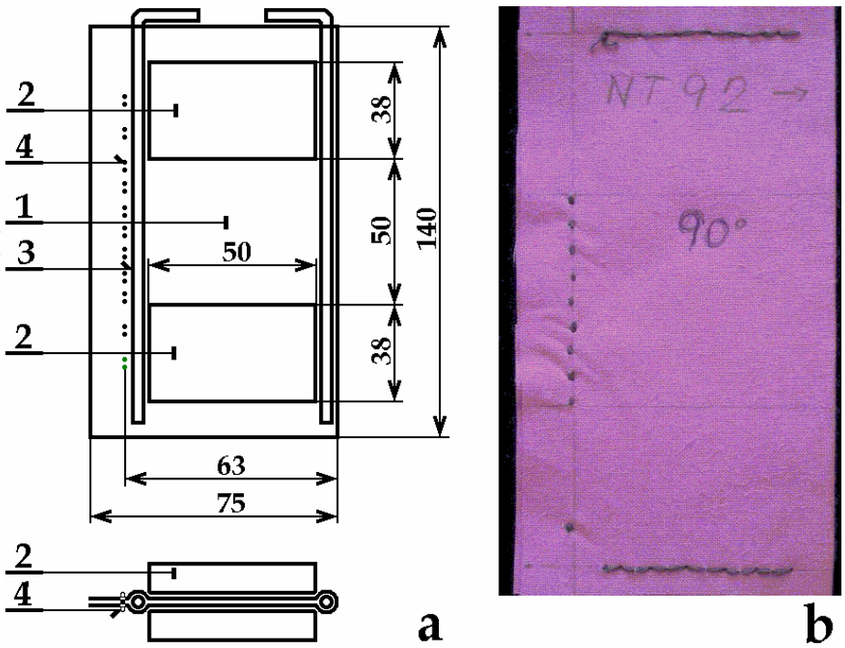

Fig. 19. Measuring of tensile properties at restricted lateral contraction (scheme, sample)

c. Development of suitable experimental methods and its standardization; till now there is no standard method for measuring rupture properties of fabrics with great lateral contraction.
d. Implementation of other variable parameters into calculation, such as variability in yarns properties, unevenness of fabric structure etc.
e. Research of another weaves (twill, sateen…), influence of structure on utilization of strength of used fibres.
f. Developing of suitable methods for simulation of fabric tension distribution at particular load with the stress to be put on a great and variable Poison's ratio of fabrics etc.

There are other important anisotropic forms of fabric deformation, which are not described in this chapter, such as bend (Cassidy & Lomov, 1998) and shear. Lateral contraction is as well very important.

6. Acknowledgement

This work was supported by the research project No. 106/09/1916 of GACR (Grant Agency of Czech Republic).

7. References

Bassett, R. J.; Postle, R. & Pan, N. (1999). Grip Point Spacing Along the Edges of an Anisotropic Fabric Sheet in a Biaxial Tensile Test. *Polymer composites*, Vol. 20, No. 2

Cassidy, C. & Lomov, S. V. (1998). Anisotropy of fabrics and fusible interlinings. *International Journal of Clothing Science and Technology*, Vol. 10 No. 5, pp. 379-390

Dai, X.; Li, Y. & Zhang, X. (2003). Simulating Anisotropic Woven Fabric Deformation with a New Particle Model, *Textile Res. J.* 73 (12), 1091-1099

Dolatabadi, K. M.; Kovar, R. & Linka, A. (2009). Geometry of plain weave fabric under shear deformation. Part I: measurement of exterior positions of yarns. *J. Text. Inst.*, 100 (4), 368-380

Dolatabadi, K. M. & Kovar, R. (2009). Geometry of plain weave fabric under shear deformation. Part II: 3D model of plain weave fabric before deformation and III: 3D model of plain weave fabric under shear deformation. *J. Text. Inst.*, 100 (5), 381-300

Du, Z., & Yu, W. (2008). Analysis of shearing properties of woven fabrics based on bias extension, *J. Text. Inst.*, 99, 385-392

Hearle, J. W. S.; Grosberg, P. & Backer, S. (1969). *Structural Mechanics of Fibres, Yarns and Fabrics*. Vol. 1. New York, Sydney, Toronto

Hofstee, J. &van Keulen, F. (2000). Elastic stiffness analysis of a thermo-formed plain-weave fabric composite. Part II: analytical models. *Composites Science and Technology*, 60, 1249-1261

Hu, J. (2004). *Structure and mechanics of woven fabrics*. Woodhead Publishing Ltd. P 102, ISBN 0-8493-2826-8

Kilby, W. F. (1963). Planar stress-strain relationships in woven fabrics. *J. Text. Inst.*, 54, T 9-27

King, M. J.; Jearanaisilawong, P. & Socrate, S. (2005). A continuum constitutive model for the mechanical behavior of woven fabrics. *International Journal of Solids and Structures* 42, 3867–3896

Kovar, R. & Gupta, B. S. (2009). Study of the Anisotropic Nature of the Rupture Properties of a Woven Fabric. *Textile Research Journal* Vol 79(6), pp. 506-506

Kovar, R. & Dolatabadi, M. K. (2010). The way of measuring of textile fabric deformation and relevant equipment. Czech patent No. 301 314

Kovar, R. & Dolatabadi, M. K. (2008). Crimp of Woven Fabric Measuring. Conference Strutex 2008, TU of Liberec 2008, ISBN 978-80-7372-418-4

Kovar, R. & Dolatabadi, M. K. (2007). Impact of yarn cut ends on narrow woven fabric samples strength. Strutex, TU Liberec, ISBN 978-80-7372-271-5

Kovar, R. (2003). *Structure and properties of flat textiles* (in Czech). TU of Liberec, ISBN 80-7083-676-8, Liberec, CZ, 142 pages

Lo, M. W. & Hu, J. L. (2002). Shear Properties of Woven Fabrics in Various Directions, *Textile Res. J.* 72 (5), 383-390

Lomov, S. V. et all, (2007) Model of internal geometry of textile fabrics: Data structure and virtual reality implementation. *J. Text. Inst.*, Vol. 98, No. 1 pp. 1–13

Pan, N. & Yoon, M. Y. (1996). Structural Anisotropy, Failure Criterion, and Shear Strength of Woven Fabrics. *Textile Res. J.* 66 (4), 238-244

Pan, N. & Yoon, M. Y. (1993). Behavior of Yarn Pullout from Woven Fabrics: Theoretical and Experimental. *Textile Res. J.* 63 (1), 629-637

Pan, N. (1996 b). Analysis of Woven Fabric Strength: Prediction of Fabric Strength Under Uniaxial and Biaxial Extension, *Composites Scence and Technology* 56 311-327

Peng, X. Q. and Cao, J. (2004). A continuum mechanics-based non-orthogonal constitutive model for woven composite fabrics. *Composites: Part A* 36 (2005) 859–874

Postle, R.; Carnaby, G. A. & de Jong, S. (1988). The Mechanics of Wool Structures. Ellis Horwood Limited Publishers, Chichester. ISBN 0-7458-0322-9

Sun, H. & Pan, N. (2005 a). Shear deformation analysis for woven fabrics. *Composite Structures* 67, 317–322

Sun, H. & Pan, N. (2005 b). On the Poisson's ratios of a woven fabric. University of California Postprints, Paper 662

Zborilova, J. & Kovar, R. (2004). Uniaxial Woven Fabric Deformation. Conference STRUTEX, TU of Liberec, pp. 89-92, ISBN 80-7083-891-4

Zheng, J. et all (2008). Measuring technology of the Anisotropy Tensile Properties of Woven Fabrics. *Textile Res. J.*, 78, (12), pp. 1116-1123

Zouari, R., Amar, S. B. & Dogui, A. (2008). Experimental and numerical analyses of fabric off-axes tensile test. *JOTI*, Vol. 99, iFirst 2008, 1–11

European standard EN ISO 13934-1. Determination of maximum force and elongation at maximum force using the strip method

CSN standard 80 0810 Zistovanie trznej sily a taznosti pletenin (Recognition of breaking stress and strain of knitted fabrics)

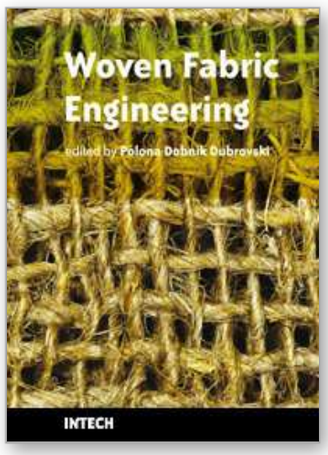

Woven Fabric Engineering

Edited by Polona Dobnik Dubrovski

ISBN 978-953-307-194-7
Hard cover, 414 pages
Publisher Sciyo
Published online 18, August, 2010
Published in print edition August, 2010

The main goal in preparing this book was to publish contemporary concepts, new discoveries and innovative ideas in the field of woven fabric engineering, predominantly for the technical applications, as well as in the field of production engineering and to stress some problems connected with the use of woven fabrics in composites. The advantage of the book Woven Fabric Engineering is its open access fully searchable by anyone anywhere, and in this way it provides the forum for dissemination and exchange of the latest scientific information on theoretical as well as applied areas of knowledge in the field of woven fabric engineering. It is strongly recommended for all those who are connected with woven fabrics, for industrial engineers, researchers and graduate students.

INTECH
open science | open minds

InTech Europe
University Campus STeP Ri
Slavka Krautzeka 83/A
51000 Rijeka, Croatia
Phone: +385 (51) 770 447
Fax: +385 (51) 686 166
www.intechopen.com

InTech China
Unit 405, Office Block, Hotel Equatorial Shanghai
No.65, Yan An Road (West), Shanghai, 200040, China
中国上海市延安西路65号上海国际贵都大饭店办公楼405单元
Phone: +86-21-62489820
Fax: +86-21-62489821

IntechOpen